Conference Paper, Published Version

Maza, Maria; Lara, Javier L.; Losada, Iñigo J.

Flow Interaction with Natural Structures: a Case Study of a Model Rhizophora Forest

Coastal Structures 2019 - Nils Goseberg, Torsten Schlurmann (eds) - © 2019 Bundesanstalt für Wasserbau
ISBN 978-3-939230-64-9 (Online) - DOI: 10.18451/978-3-939230-64-9_103

Flow Interaction with Natural Structures: a Case Study of a Model Rhizophora Forest

M. Maza, J. L. Lara & I. J. Losada
Environmental Hydraulic Institute "IHCantabria", Univ. de Cantabria, Spain

Abstract: An experimental analysis of flow interaction with a model 26 m long Rhyzophora mangrove forest is performed. Mangrove trees are built representing a mature Rhyzophora forest and a 1:6 scale is considered to fit the forest into the flume. Scaled random wave conditions representative of these environments are tested. Results reveal a strong influence of the facility induced friction in the overall obtained wave height attenuation. This additional damping produced by bottom and walls friction should be considered in order to properly evaluate the attenuation capacity of the mangrove trees. The analytical drag forces obtained from wave attenuation analysis agree well with measured forces within the forest when damping induced by bottom and walls friction is subtracted. These analytical forces can then represent a first estimate of the drag force used in several analytical or numerical models to quantify the wave attenuation capacity produced by mangrove trees.

Keywords: coastal protection, wave attenuation, drag forces, Rhizophora mangrove, large 3-D model

1 Introduction

Mangrove forests grow in intertidal areas in the tropical zones and they are characterized by their complex root system, specially red mangroves as Rhizophora species. The capacity of these ecosystems to reduce the incoming flow energy has already been proven (e.g.: Mazda et al. 1997; Narayan et al., 2016). Additionally, these ecosystems provide with other ecosystem services, such us increase biodiversity, improve water quality or capture CO2 (Barbier et al. 2011). Due to all these aspects, Nature Based Solutions, solutions for coastal protection based on ecosystems, have become an interesting option to mitigate and adapt to Climate Change.

Although mangroves reduce annual flooding to millions of people (Menéndez et al., 2018) there is not a methodology to implement these solutions and it is still difficult to estimate the protection provided by them under different environmental conditions and ecosystem properties. To move forward in the consecution of an engineering approach when implementing these solutions the first step to make is to better understand and parameterize the basic physical processes involved in flow-mangroves interaction. Several studies have been performed in the last decade to characterize flow interaction with mangrove trees, trying to reproduce the complex geometry of these ecosystems (e.g.: Strusinska-Correia et al., 2013; Zhang et al., 2015; Maza et al. 2017). However, these studies have been performed at small scales without considering, in most of the cases, any similarity to define flow conditions and testing unidirectional flow or solitary waves. Thus, there is still a lack of knowledge of the attenuation rates and the forces exerted on the trees associated to different wave conditions. This understanding is key when designing restoration projects and when quantifying the coastal protection capacity of these ecosystems.

To further investigate these aspects an experimental campaign is carried out where both wave attenuation and forces on the individuals are measured under different wave conditions. Section 2 details the experimental set-up. Results are presented in Section 3 and the most relevant conclusions are drawn in Section 4.

2 Experimental set-up

A model mangrove forest is built following the parameterization given by Ohira et al. (2013) and Maza et al. (2017). A mature Rhizophora forest is considered, leading to mangrove models formed by 24 roots distributed in a three dimensional layout and connected to the vertical main trunk at different heights, being the highest root at 2.012 m at real scale. The diameter of these roots range from 0.033 to 0.042 m. A mean diameter equal to 0.037 m is considered to build all the roots. The scale used in the experiments is 1:6, sufficient to fit the forest into the Cantabria wave-current-tsunami flume (COCOTSU) at IHCantabria. 135 trees are built leading to a mangrove forest 26 m long (Figure 1), representing 156 m at real scale. 56 of these trees are half trees to be able to locate them next to the flume walls to avoid preferable channels. The models are built using a PVC tube of 0.03 m of diameter for the trunk and aluminum rods of 0.006 m of diameter for the roots. The tallest root is at 0.33 m at laboratory scale. The main trunk of the models has an extra length at the bottom to insert them into waterproof baseboards that are fixed to the bottom of the flume. In these baseboards, holes slightly smaller than the diameter of the trunk are drilled.

The forest density chosen in these experiments is equal to 625 trees/ha at real scale and they are distributed following a staggered arrangement as is shown in Figure 1. To reproduce a fringe mangrove forest the study area is located on a flat bottom placed after a 1:13.5 slope that features the seaward slope in front of the forest. The first row of mangroves is located 1 m after the end of this 4.7 m long slope.

Fig. 1. Mangrove forest set-up. Views of the 26 m long forest with staggered configuration.

Random waves are tested over three water depths, h = 0.17, 0.33 and 0.50 m, that correspond to values below, at and above the location of the highest root. Wave conditions are chosen based on wave heights and periods found in these ecosystems (i.e.: Bao, 2011, Brinkman 2006) and using Froude similarity to scale them. Reynolds similarity is also considered to ensure that wake structures shedding from the trunk and the roots are the same as the ones found in the field. Thus, Reynolds numbers for scaled conditions are larger than 600 ensuring a turbulent wake. Selected significant wave heights, H_S, range from 0.04 to 0.15 m and peak wave periods, T_p, from 1.44 to 2.64 s. A total of 44 tests are performed. Table 1 shows the tests performed for each water depth. 300 waves are

generated for each condition. All tests are run twice, once with the mangrove forest located inside the flume and once without the mangroves. This allows estimating the dissipation of energy induced by the walls and bottom friction of the flume.

Tab. 1. Random wave conditions for the three water depths.

Test	h = 0.17 m		Test	h = 0.33 m		Test	h = 0.50 m	
	H_S(m)	T_p (s)		H_S(m)	T_p (s)		H_S(m)	T_p (s)
1- 4	0.04	1.44, 1.92, 2.40, 2.64	1- 4	0.04	1.44, 1.92, 2.40, 2.64	1- 4	0.04	1.44, 1.92, 2.40, 2.64
5 - 8	0.06	1.44, 1.92, 2.40, 2.64	5 - 8	0.06	1.44, 1.92, 2.40, 2.64	5 - 8	0.06	1.44, 1.92, 2.40, 2.64
			9 - 12	0.09	1.44, 1.92, 2.40, 2.64	9 - 12	0.09	1.44, 1.92, 2.40, 2.64
			13 - 16	0.12	1.44, 1.92, 2.40, 2.64	13 - 16	0.12	1.44, 1.92, 2.40, 2.64
						17 - 20	0.15	1.44, 1.92, 2.40, 2.64

Free surface is measured at 31 locations along the flume including 3 gauges offshore the forest and 3 onshore. Figure 2 shows the location of the 25 gauges located along the forest. Flow exerted forces on the mangroves are recorded at 9 mangroves located at the first half part of the forest using a new arm developed to improve the design presented by Maza et al. (2017). This new arm consists of a frictionless rotating point connecting the mangrove model to a load cell. The mangrove model is hold by the arm without touching the flume floor allowing its free motion under the flow action. The model is hold at one end of the arm whereas the load cell is located at the other end being the frictionless point in between them. After the calibration of the load cell is performed, it is compressed or pulled under the flow action and the force exerted on the mangrove model is recorded. A sketch of this arm is shown in Figure 2.

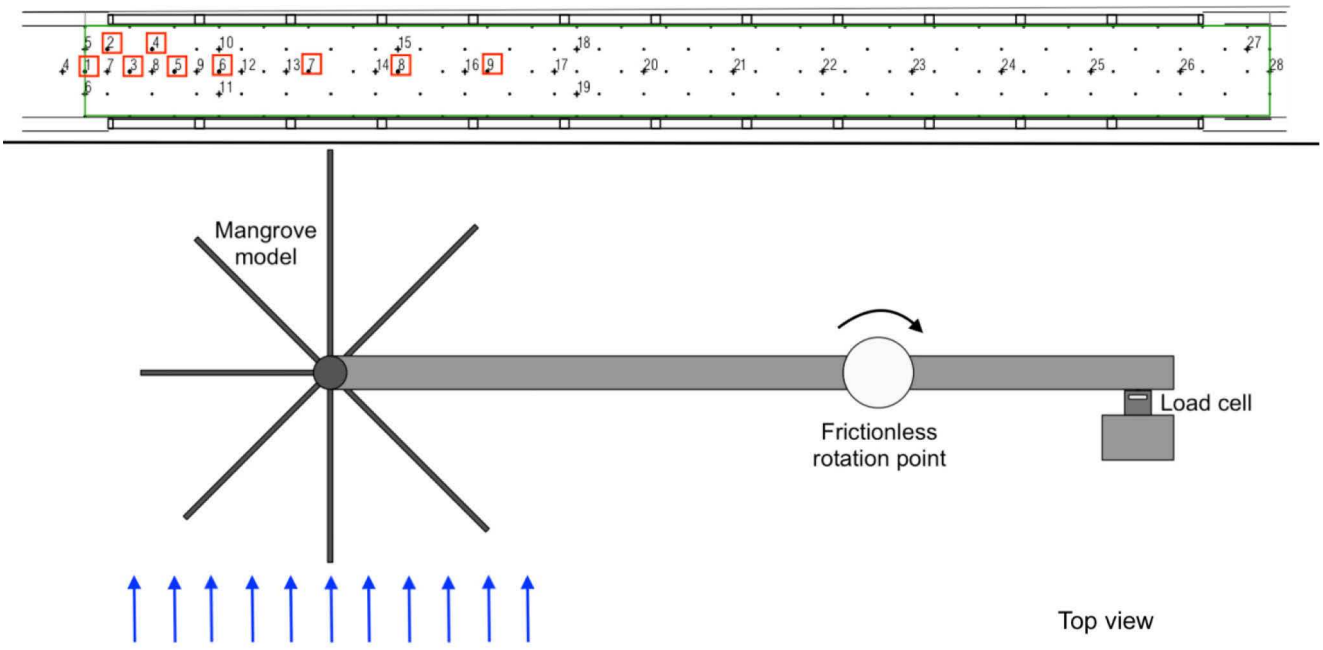

Fig. 2. Upper panel: top view of the flume. Free surface gauges (black crosses) and load cells (red squares) along the mangrove forest. Black dots represent the location of the models trunks and the green square limits the 26 m long forest. Lower panel: sketch of a top view of the new arm developed to measure the forces exerted by the flow on the mangrove models. Blue arrows show an example of flow direction and black arc the resultant movement around the frictionless point leading to a compression of the load cell.

3 Results

Wave height attenuation is analyzed using Mendez and Losada (2004) formulation. This widely used formula accounts for the energy attenuation produced by the vegetation by means of a damping coefficient that is fitted to the recorded root mean square wave height as follows:

$$\frac{H_{rms}}{H_{rms,i}} = \frac{1}{1+\beta X} \quad (1)$$

where H_{rms} = root mean square wave height, β = wave damping coefficient, X = distance along wave propagation direction with the origin at the frontal edge of the forest and subindex i denotes incident conditions. H_{rms} recorded by all free surface gauges are obtained and equation (1) is fitted to the data. This process is also applied to the data obtained with the empty flume to account for the energy attenuation induced by the flume walls and bottom. Figure 3 shows an example of the fittings obtained for a random wave train with H_{rms} = 0.05 m and T_p = 1.92 s for tests performed with the forest located inside the flume (M+B) and the empty flume (B) and the three water depths. Based on the β obtained for these two conditions, β_{M+B} and β_B, a new damping coefficient, β_M, is obtained by subtracting both fittings. This β_M accounts for the damping induced by the mangrove models by eliminating the damping induced by the facility.

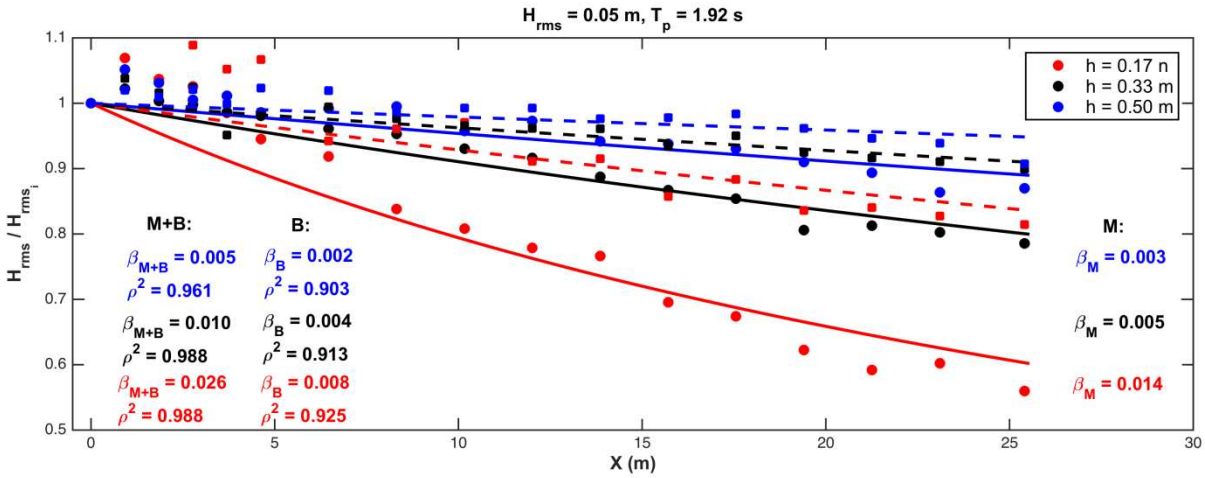

Fig. 3. Root mean square wave height evolution for a random wave train with H_{rms} = 0.05 m and T_p = 1.92 s over a water depth equal to 0.17 (red), 0.33 (black) and 0.50 (blue) m. Results for tests performed with the flume full of mangroves are presented in circles and the associated fitting in solid line. Results for tests run with the empty flume are presented in squares and dashed lines. Associated β for tests with the mangrove forest (M+B), for the empty flume (B) and the resultant β quantifying the action of the mangrove models (M) are also displayed in the figure. Correlation coefficients for each fit, ρ^2, are displayed.

Figure 3 shows an increase of wave height along the first meters of the forest. This increase is also observed for the tests performed with the empty flume. Then, this is a local effect produced by the seaward slope. Thus, seaward slope in fringe mangroves produces shoaling and can lead to a local increase in the wave height along the first meters of the forest. The non-uniform vertical frontal area, characteristic of these mangrove forests, strongly influences wave attenuation and the highest attenuation rates are obtained for the smallest water depth. Figure 3 also reveals the highest dissipation induced by the bottom and walls friction for the smallest water depth and the strong influence that this friction can have in the resultant damping coefficients. Then, it is very important to consider this additional friction induced by the facility when running experiments to quantify the wave damping induced by an ecosystem.

To further explore this fact, analytical drag forces are evaluated from the obtained wave damping coefficients. Mendez and Losada (2004) formulation relating the damping coefficient to the drag coefficient is used to evaluate the second:

$$C_D = \frac{3\sqrt{\pi}}{dNH_{rms,i}k} \frac{(sinh2kh+2kh)sinhkh}{sinh^3kl+3sinhkl} \beta \quad (2)$$

where C_D= drag coefficient, d = mangrove area per unit height, N = number of mangroves per square meter, k = wave number and l = submerged length of the mangroves. This formulation is applied to get C_D and then the drag force is evaluated as:

$$F_D = \frac{1}{2}\rho A_f C_D U|U| \quad (3)$$

where F_D = drag force, ρ = fluid density, A_f = mangrove frontal area and U = depth averaged wave velocity under the wave crest. Then, the force exerted on a mangrove model is evaluated analytically using equations (2) and (3) considering β_{M+B} and β_M. This allows comparing the analytical forces obtained before and after subtracting the walls and bottom friction to the measured ones and thus verify which of the two provides a better estimate.

Dynamic forces recorded in the laboratory are analyzed to get the maximum, F_{max}, and the root mean square, F_{rms}, force exerted on each of the nine mangrove models. Figure 4 shows these forces for a tests with H_{rms} = 0.05 m and T_p = 1.92 s for the three water depths. As can be observed in Figure 4, for the same wave conditions the maximum dynamic forces are obtained for the smallest water depth where the frontal area of the model and the depth averaged velocity are the highest. An increase is observed along the first meters of the forest in agreement with the increase in wave height observed in Figure 3. Forces recorded in mangroves 7, 8 and 9 reveal small variations.

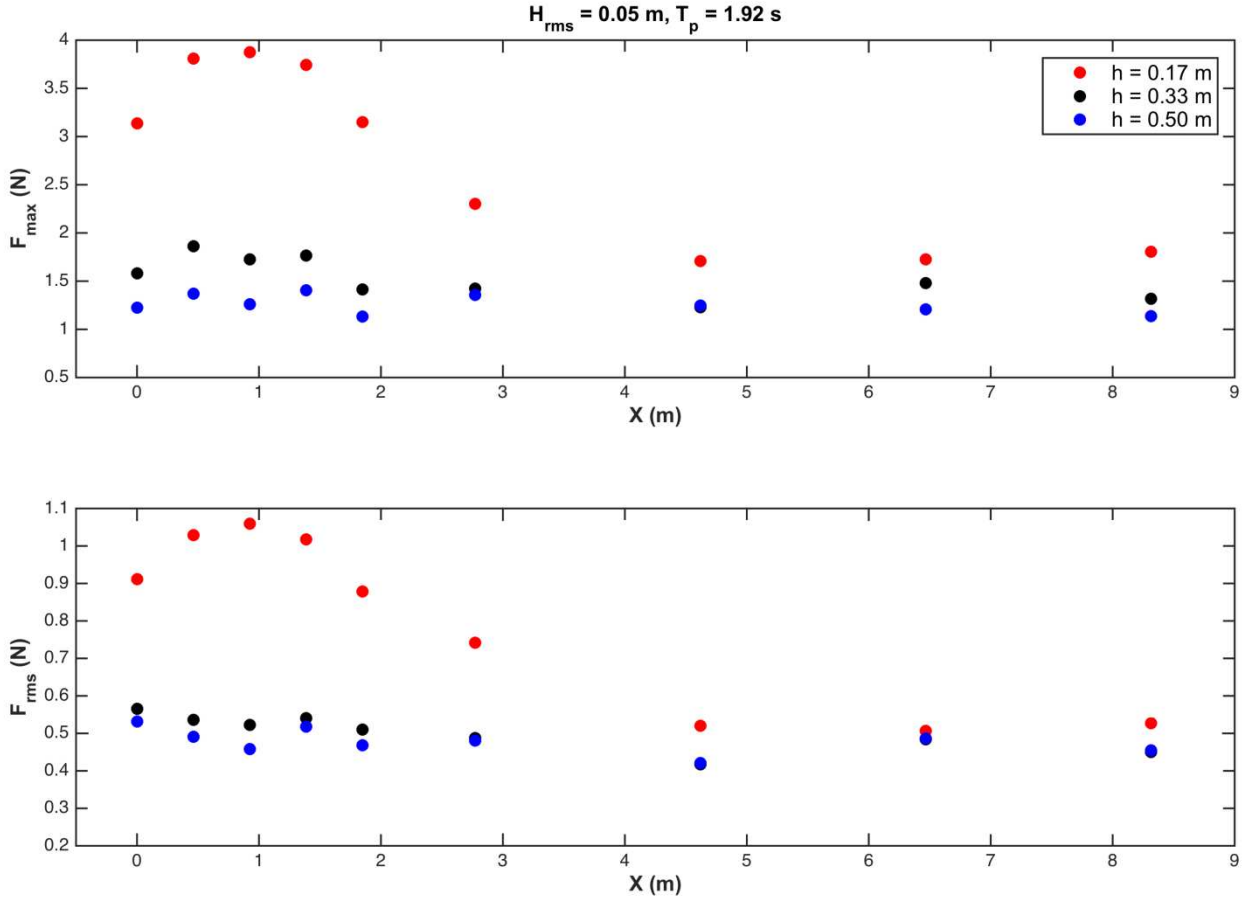

Fig. 4. Maximum, F_{max}, and root mean square, F_{rms}, forces recorded on the nine mangrove models marked in red in Figure 2 for a wave train with H_{rms} = 0.05 m and T_p = 1.92 s and the three water depths: 0.17 (red), 0.33 (black) and 0.50 (blue) m.

Analytical forces obtained using Equations (2) and (3) and coefficients β_{M+B} and β_M are compared to the measured values. Measured F_{rms} is considered since analytical forces are obtained based on Mendez and Losada (2004) formulation that is derived in terms of H_{rms}. Additionally, F_{rms} recorded in mangrove model 9 are considered for the comparison as Equation (1) fits better to the measured data after the first meters of the forest where wave height increases. Therefore, F_{rms} recorded in mangrove 9 is compared to the analytical forces obtained using β_{M+B} and β_M as a function of the Reynolds number, Re. Re is obtained as:

$$Re = \frac{dU}{\nu} \quad (4)$$

where ν = kinematic viscosity. Figure 5 shows this comparison for all tests performed over the three water depths.

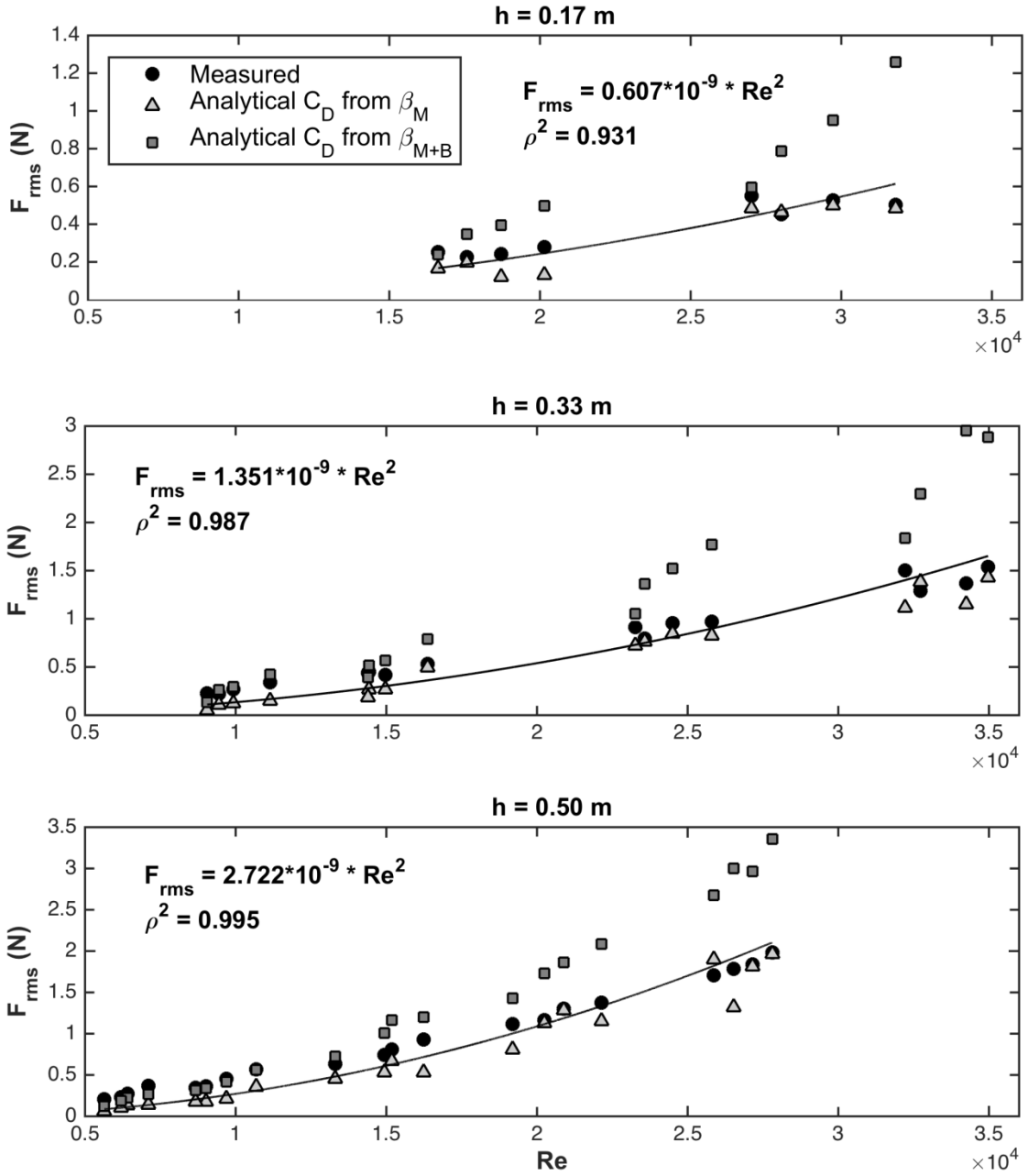

Fig. 5. Comparison of root mean square force measured in the laboratory (black circles) to the analytical forces obtained by using β_M and β_{M+B} and equations 2 and 3. Results are plotted as a function of Re. The quadratic relationship found between measured forces and Re is also displayed in the figure by a solid line and the associated equation is shown.

Analytical forces obtained using β_M, that is, the damping coefficient obtained after subtracting the dissipation induced by the flume walls and bottom, agree well with the measured F_{rms} recorded in mangrove model 9, as can be observed in Figure 5. However, if this additional dissipation produced by the facility is not subtracted the obtained drag forces overestimates the measured values. This confirms the necessity of considering the wave attenuation induced by the facility when quantifying the attenuation capacity of the ecosystem. A quadratic relationship between the measured F_{rms} and the Re is obtained for the three water depths. Figure 5 shows this fitting and the associated equation revealing high correlation coefficients, $\rho^2 > 0.9$ for all cases.

4 Conclusions

An experimental study of wave interaction with a 26 m long Rhyzophora mangrove forest is presented here. The forest is built representing a mature Rhyzophora fringe forest. Random wave trains representative of field conditions in these environments are tested over three water depths. Free surface and forces exerted on different mangrove models along the forest are measured. Tests are performed twice: once with the empty flume and once with the forest located inside it. This allows quantifying the effect of bottom and walls friction.

Wave height attenuation analysis shows an initial increase of the wave height due to the shoaling effect produced along the seaward slope of the fringe forest. This increase vanishes after the first few meters of the forest and Mendez and Losada (2004) formulation for wave damping fits well to the measured data. Wave damping analysis reveals a strong influence of bottom and walls friction. Wave damping coefficients obtained before, β_{M+B}, and after subtracting the contribution of bottom and walls friction, β_M, differ significantly. Then, the attenuation capacity of the mangrove trees can be overestimated if the damping induced by the facility is not considered. At real environments, bottom friction also plays a role in the total attenuation capacity of the ecosystem. However, the friction induced by the laboratory facility cannot be considered representative of this natural soil friction. Then, β_M can be combined to additional friction assessed for the characteristic soil of the area to obtain a representative value of the attenuation capacity of the entire ecosystem.

Wave dynamic drag forces analysis confirms the good estimation of the mangrove trees attenuation capacity after subtracting the facility induced friction. Analytical forces obtained by using β_M agree well with the measured F_{rms} inside the forest. Several analytical and numerical models in the literature dealing with wave attenuation induced by ecosystems are based on a drag force introduced into the momentum equation. Then, β_M obtained from wave height attenuation analysis can serve as an initial estimation of this force when direct measurements of the exerted forces are not available. However, direct measurements of the exerted forces on the individual trees are needed to well reproduced local effects, such as the one observed here along the first meters of the forest due to wave shoaling along the seaward slope.

Acknowledgements

This work has been funded under the RETOS INVESTIGACION 2014 (grant BIA2014-59718-R) program of the Spanish Ministry of Economy and Competitiveness. M. Maza is indebted to the Spanish Ministry of Science, Innovation and Universities for the funding provided in the grant Juan de la Cierva Incorporación (BOE de 27/10/2017).

References

Barbier, E.B., Hacker, S.D., Kennedy, C., Koch, E.W., Stier, A.C., Silliman, B.R., 2011. The value of estuarine and coastal ecosystem services. Ecol Monogr., 81, 169-193.

Maza, M., Adler, K., Ramos, D., Garcia, A., Nepf, H., 2017. Velocity and drag evolution from the leading edge of a model mangrove forest. Journal of Geophysical Reseach (JGR) - Oceans, 122.

Mazda, Y., Magi, M., Kogo, M., Hong, P.M., 1997. Mangrove as a coastal protection from waves in the Tong King delta, Vietnam. Mangroves Salt Marshes, 1: 127-135.

Mendez, F.J., Losada, I.J., 2004. An empirical model to estimate the propagation of random breaking and non-breaking waves over vegetation fields. Coastal Engineering, 52, 103 – 118.

Menéndez, P., Losada, I.J., Beck, M.W., Torres-Ortega, S., Espejo, A., Narayan, S., Díaz-Simal, P., Lange, G.-M., 2018. Valuing the protection services of mangroves at national scale: The Philippines. Ecosystem Services, 34, 24-36.

Narayan, S., Beck, M.W., Reguero, B. G., Losada, I.J., van Wesenbeeck, B., Pontee, N., Sanchirico, J.N., Ingram, J.C., Lange, G.M., Burks-Copes, K.A., 2016. The effectiveness, Costs and Coastal Protection Benefits of Natural and Nature-Based Defenses. PLos ONE, 11(5), e0154735.

Ohira, W., Honda, K., Nagai, M., Ratanasuwan, A., 2013. Mangrove stilt root morphology modelling for estimating hydraulic drag in tsunami inundation simulation. Trees, 27, 141-148.

Strusinska-Correia, A., Husrin, S., Oumeraci, H., 2013. Tsunami damping by mangrove forest: a laboratory parameterized trees. Nat. Hazards Earth Syst. Sci., 13, 483-503.

Zhang, X., Chua, V.P., Cheonf, H.F., 2015. Hydrodynamics in mangrove prop roots and their physical properties. Journal of Hydro-environment Research, 9, 281-294.